Hindawi Publishing Corporation
Journal of Nanomaterials
Volume 2015, Article ID 842365, 9 pages
http://dx.doi.org/10.1155/2015/842365

Research Article

Green Synthesis of $CuInS_2$/ZnS Nanocrystals with High Photoluminescence and Stability

Min Fu,[1,2] Weiling Luan,[1] Shan-Tung Tu,[1] and Leslaw Mleczko[3]

[1]*Key Laboratory of Pressure Systems and Safety (MOE), School of Mechanical and Power Engineering, East China University of Science and Technology, Shanghai 200237, China*
[2]*Technology Development, Bayer Technology and Engineering (Shanghai) Co. Ltd., Shanghai 201507, China*
[3]*Technology Development, Bayer Technology Services GmbH, 51368 Leverkusen, Germany*

Correspondence should be addressed to Weiling Luan; luan@ecust.edu.cn

Received 15 March 2015; Accepted 30 August 2015

Academic Editor: Mohamed Bououdina

Copyright © 2015 Min Fu et al. This is an open access article distributed under the Creative Commons Attribution License, which permits unrestricted use, distribution, and reproduction in any medium, provided the original work is properly cited.

Highly photoluminescent core/shell $CuInS_2$/ZnS (CIS/ZnS) nanocrystals were synthesized. Zinc acetate and dodecanethiol in octadecene solvent were used for shell growth. The structure and composition of QDs were investigated with inductively coupled plasma-optical emission spectroscopy, X-ray photoelectron spectroscopy, and transmission electron microscopy. The crystal phase of CIS was tetragonal chalcopyrite. Based on X-ray diffraction analysis, it has been concluded that the growth of the ZnS shell did not affect the phase structure of $CuInS_2$ (CIS). Photoluminescence (PL) quantum yield (QY) of CIS increased to 80% after epitaxial growth of ZnS, and the PL emission wavelength can be feasibly tuned to be in the range of 560–710 nm by adjusting shell growth time. The superb photostability with high PL QY of CIS/ZnS nanocrystals is ascribed to the gradient of the chemical composition that has been formed between the core and the shell.

1. Introduction

Semiconducting nanocrystals or quantum dots (QDs) are characterized by a quantum confinement of electron and hole in all three dimensions, which leads to an increase in the effective band gap of the material and shifts of both the optical absorption and emission of semiconducting QDs depending on the particle size; larger particles display smaller band gaps while smaller particles show larger band gaps. QDs can be applied in the fields of flexible solar cells [1], thermoelectric devices [2], light emitting diodes (LED) [3, 4], liquid crystal molecules (LCD) [5], sensors [6], fluorescent probes [7–9], biolabeling [10], anticounterfeiting [11], lasers [12–14], and so forth. Some of these QDs are CdSe [15], CdTe [16], CdS [17], PbSe [18], and $FeSe_2$ [19]. However, most of these semiconductors contain toxic heavy metals such as Cd, Pb, and Te, which limits their application in consumer products. Consequently, many researchers turned their attention to alternative nontoxic or minimally toxic semiconductor compounds. Ternary semiconductors based on IB, IIIA, and VIA elements of the periodic classification (I-III-VI_2 type semiconductors) including $CuInS_2$ (CIS), $CuInSe_2$ (CISe), $AgInS_2$ (AIS), and $CuGaS_2$ (CGS) have shown promising results for applications in these fields. Among these semiconductors, CIS semiconductors have been receiving considerable attention because of their low toxicity, high energy conversion efficiency, high light absorption coefficient ($\alpha \approx 10^5$ cm^{-1}) [20], and low production cost, which are desired properties for photovoltaic applications.

Various approaches have been reported for CIS synthesis including solvothermal synthesis [21], single-source precursor routes [22], and hot injection techniques [23], which can produce high quality CIS QDs based on monodispersity, crystallinity, and high photoluminescence efficiency. However, the photoluminescence (PL) quantum yield (QY) is usually lower than 10%, which is still far from commercial application. Furthermore, the PL efficiency is not stable and QDs are sensitive to air [24, 25]. In order to overcome these

obstacles, several concepts aiming at modification of the crystal surface have been proposed. For example, CIS-ZnS alloyed QDs were synthesized by diffusing Zn into CIS seeds at high temperatures in solution so the QY could reach 39% [26]. Xie et al. prepared CIS/ZnS using S as an anion source and the reaction was carried out below 200°C with a maximum QY around 30%. Photostability of CIS was significantly improved when coating it in ZnS by sitting in air condition for several months [25]. Li et al. used zinc ethylxanthate as a Zn source, dodecanethiol, DMF, ODE, and toluene (added in a shell formation step), achieving a high QY around 60% [27]. Li et al. reported the record value of 67% QY of CIS/ZnS and 86% QY of CIS/CdS QDs, in which the shell was generated by reaction of zinc stearate (or cadmium oleate) with S in trioctylphosphine (TOP) and octadecene (ODE) solution [28]. Recently, Zhang et al. synthesized hydrophilic CIS/ZnS QDs with a maximum PL QY of 9% by using *in situ* generated H_2S as the sulphur source, DMF as the solvent, and 1-thioglycerol as the capping ligands. The photostability of CIS/ZnS was increased relative to bare CIS QDs, but the PL efficiency decreased rapidly after the first week due to the surface oxidation [24]. Although significant progress has been made in the preparation of shell-coated CIS QDs, there are still some issues to be addressed. For example, a blue shift occurs during the process of ZnS shell growth around the CIS QDs, which has also been noted in previous work [21, 27–29]. Different reasons for this behavior have been suggested, such as interdiffusion of Zn atoms [21], surface reconstruction [27], etching of the plain core material [28], and cation exchange [29]. Moreover, the CIS-based QDs with the highest QY to our knowledge were synthesized based on the growth of toxic CdS, which limits its future applications.

In this work, a simple synthetic process for the growth of ZnS on CIS surface was developed in order to improve PL efficiency of CIS QDs. During the synthesis, CIS core QDs were prepared based on the recipe published in the literature [25]; ZnS precursor containing zinc acetate, dodecanethiol (DDT), and octadecene (ODE) was then injected into the same reactor with existing CIS cores that have not been purified for ZnS shell growth. DDT was used as the S source as well as a capping ligand. This is a green, simple, and economical method to obtain highly luminescent and structurally stable QDs for the following reasons: only affordable and nontoxic materials were used in the synthesis; the solvent, S source, and ligand used in the shell growth step were the same as those in the CIS core synthesis, which simplified the separation steps in postprocess treatment and saves cost in large scale production.

2. Experimental

2.1. Chemicals. Zinc acetate ($Zn(Ac)_2$, 99.9%) was purchased from Tokyo Chemical Industry Co., Ltd. Copper (I) acetate (CuAc, 99%) and indium acetate ($In(Ac)_3$, 99.99%) were purchased from ABCR. Dodecanethiol (DDT, 97%) was purchased from Acros. Octadecene (ODE, 90%) was purchased from Alfa. All chemicals were directly used without further purification.

2.2. Synthesis of CIS QDs. $Zn(Ac)_2$ (0.60 mmol) and $In(Ac)_3$ (0.60 mmol) were mixed with 15 mL of ODE and 1.5 mL of DDT in a 100 mL three-neck flask under N_2 atmosphere. The mixture was degassed for 30 min under magnetic stirring and then heated to 240°C for reaction. The heating source was removed to stop the reaction after set time and crude CIS solution was obtained. Three equivalents of an acetone/isopropanol mixture (1/4 by v/v) were added to the crude CIS solution, and then CIS QDs were separated by centrifugation at 9000 rpm for 20 min. The CIS QDs were then redispersed in toluene, rinsed with the acetone/isopropanol mixture, and then separated at least twice more in order to eliminate byproducts, unreacted starting reagents, and excess ligand and solvent.

2.3. Synthesis of Core/Shell CIS/ZnS QDs. The Zn-precursor solution was prepared by dissolving a certain amount of $Zn(Ac)_2$ (Zn/Cu feeding molar ratio is in the range of 1–16) in mixture of 3 mL of DDT and 6 mL of ODE. Without an intermediate purification step of the CIS QDs, the ZnS precursor solution was rapidly added into the crude CIS solution and the temperature was adjusted for shell growth without any purification. The shell growth temperature was tuned in the range of 220~240°C. Separation and purification of obtained core/shell CIS/ZnS QDs were carried out in the same way as described for CIS QDs.

2.4. Characterization. UV-vis absorption spectra of CIS and core/shell CIS/ZnS QDs were measured by UV-vis spectrophotometer (Varian, USA). The samples were diluted by toluene until the absorption values of the QDs were around 0.05 at 485 nm. The PL spectra of the QDs were measured by spectrofluorometer (Cary Eclipse, Varian, USA) at excitation wavelength of 485 nm. QYs of the samples were determined by comparing their integrated emissions with those of standard dye of rhodamine B with a known QY of 97% in an ethanol solution. The samples were diluted in toluene following the measurement rules of UV-vis and PL spectra. The QYs of samples were determined according to

$$Y_Q = Y_S \times \frac{F_Q}{F_S} \times \frac{A_S}{A_Q} \times \frac{{D_Q}^2}{{D_S}^2}, \quad (1)$$

wherein Y_Q refers to the QY of obtained samples; Y_S refers to the QY of standard dye of rhodamine B; F_Q and F_S represent the integral intensity under PL spectrum of samples and rhodamine B, respectively; A_Q and A_S are the absorption values at the excitation wavelength of samples and rhodamine B, respectively; D_Q and D_S refer to the refractive index of the corresponding solvent of samples and rhodamine B. The crystal phase of samples was obtained by X-ray diffraction devices (XRD, Rigaku Corporation, and D/max-2200/PC). The X-ray source used was Cu/Kα (40 KV, 30 mA). The shape and size of the samples were observed using TEM (CM20, Philips). The samples were drop-cast from a diluted dispersion in toluene onto a thin holey carbon film by a copper grid. X-ray photoelectron spectroscopy (XPS, ESCALAB 250Xi, Thermofisher Scientific) was used to analyze the shell thickness of samples and surface composition, where Al Kα was used

as the excitation source. Inductively coupled plasma-optical emission spectroscopy (ICP-OES, Varian 710ES) was used to analyze the elemental chemical composition of samples. The samples were digested in concentrated HNO_3 solutions to make a 10 ppm solution.

3. Results and Discussion

The recipe for the synthesis of CIS QDs was derived from Zhong's method [32]. During the synthesis of CIS, the Cu/In feeding molar ratio was kept at 1. The growth of shell was carried out by adding Zn-precursor solution to the above crude CIS solution with different Zn/Cu feeding molar ratio. XPS, ICP-OES, and TEM were combined to characterize the grown QDs. The results indicated that by adding Zn-precursor solution into CIS-containing solution at high temperature a core/shell structure with a gradient chemical composition between CIS core and ZnS shell has been formed. The epitaxial growth of shell was carried at 240°C for 180 min. XPS was used to measure the surface chemical composition of nanocrystals with limited depth, while ICP-OES was used to record the body chemical composition of nanocrystals. Table 1 shows the measured Zn/Cu atomic ratio by XPS and ICP-OES of samples using different Zn/Cu feeding molar ratios. The Zn/Cu atomic ratio showed the same rising tendency with the increase of the Zn/Cu feeding molar ratio. Furthermore, the value measured by XPS was usually higher than that obtained by ICP-OES. These results indicate that ZnS precipitated mainly on the CIS surface during the epitaxial growth. Photoelectron intensity variation of elements was used to show that ZnS was growing on the CIS surface as a shell. The exponential decrease of Cu and In peaks' intensities should be complemented by an exponential increase of the intensities of the Zn photoelectron peaks if ZnS only grows as a shell on the CIS. As shown in Figure 1(a), CIS QDs exhibited strong photoelectron signals with the peaks of Cu 2p, In 3d, and In Auger 3d, while in CIS/ZnS QDs Zn 2p and Zn Auger peaks gradually became more prevalent accompanied with the screening of these In- and Cu-related peaks with the increase of the Zn/Cu feeding molar ratio. Based on the above analysis, it could be concluded that ZnS coated the CIS surface and served as a shell.

XPS was used to estimate the thickness of ZnS layer. Figure 1(b) presents high resolution scans of Cu 2p photoelectrons from CIS and CIS/ZnS QDs, respectively. As reported surface structure analysis of core/shell QDs by Nam et al. on CIS/ZnS and Choi et al. on Gd_2O_3:Eu^{3+} [33, 34], the shell thickness could be approximated by using a simple principle of the exponential dependence of the core element-related photoelectron intensity on the shell thickness, which is expressed as $I/I_0 = \exp(-t/\lambda)$. Here, I/I_0 is the normalized core element-related photoelectron intensity in a core/shell particle relative to that in the core counterpart, t is the shell thickness, and λ is the attenuation distance of the photoelectron in the shell. In order to simplify the calculation, a direct core/shell structure of CIS/ZnS is assumed. The growth of a ZnS shell on CIS core was calculated by an exponential attenuation of the intensity of the Cu 2p core photoelectron peaks. I/I_0 for the Cu 2p peak was calculated from Figure 1(b) based on the Cu 2p photoelectron kinetic energy of 555 eV (binding energy of Cu 2p photoelectron: 931 eV), and λ in ZnS was estimated as ~1.2 nm [33, 34]. Figure 1(c) is the calculated thickness of ZnS shell at different Zn/Cu feeding molar ratio. The calculated averages of ZnS shell thickness are 0.5, 0.9, 2.4, and 2.8 nm at Zn/Cu feeding molar ratios of 2, 4, 8, and 16, respectively.

Table 1: Comparison of Zn/Cu atomic ratio of prepared samples by ICP-OES and XPS.

Zn/Cu feeding molar ratio	Zn/Cu atomic ratio by ICP-OES	Zn/Cu atomic ratio by XPS
2	1.5	1.7
4	3.1	4.8
8	6.3	7.0
16	13.0	18.7

TEM was used for investigation of the particle size variation of bare CIS and after adding at high temperature Zn precursor into CIS-containing solution. By analysis of the TEM images, we determined the mean diameters of bare CIS for 60 min at 240°C to be 3.3 nm (Figure 2(a)), and the particle size increased to around 4.3 nm while the shell was growing on CIS surface for 180 min at 240°C with Zn/Cu feeding molar ratio of 4 (Figure 2(b)). The thickness of the shell is estimated to be 0.5 nm by assuming a relatively uniform shell regardless of a CIS particle size. As ZnS is the supposed composition as the shell, it is around 1.5 layers based on a 0.3 nm ZnS monolayer [35]. The estimated thickness of a ZnS layer by XPS (0.9 nm) is thicker than that measured by TEM (0.4 nm) when comparing the measurement result. Since CIS and ZnS have a small lattice mismatch (2-3%) and crystallographic similarity [33], the element exchange might happen at a high growth temperature and induce the changes of CIS core size. The value gap from XPS and TEM result might be due to an additional layer that is formed between CIS core and ZnS shell.

In order to prove this assumption, the temporal evolution of element composition of CIS/ZnS QDs was measured at different growth times and compared *via* ICP-OES. The evolution of Zn/(Cu + In) and In/Cu atomic ratio as a function of the growth time of shell is shown in Figure 3. If we assume that CIS/ZnS QDs have a pure core/shell structure, the constant In/Cu atomic ratio and an increased Zn/(Cu + In) atomic ratio should be expected. As predicted, the amount of Zn/(Cu + In) ratio increased from 1.36 to 1.59 over a shell growth time of from 5 to 60 min (Figure 3(a)). However, the In/Cu value decreased from 1.28 to 0.93 as the shell growth time grew from 5 min to 60 min (Figure 3(b)), showing a trend for a Cu-rich composition in the shell, which is different from expectation. Considering the decrease of In/Cu molar ratio in epitaxial growth, parts of In^{3+} on CIS surface should be replaced by Zn^{2+} during the shell growth at high temperature, inducing the increase of ZnS thickness and shrinking of the CIS core [36]. The In^{3+} could be replaced by Zn^{2+} easily due to the small difference of Gibbs formation enthalpy and small lattice mismatch between CIS and ZnS

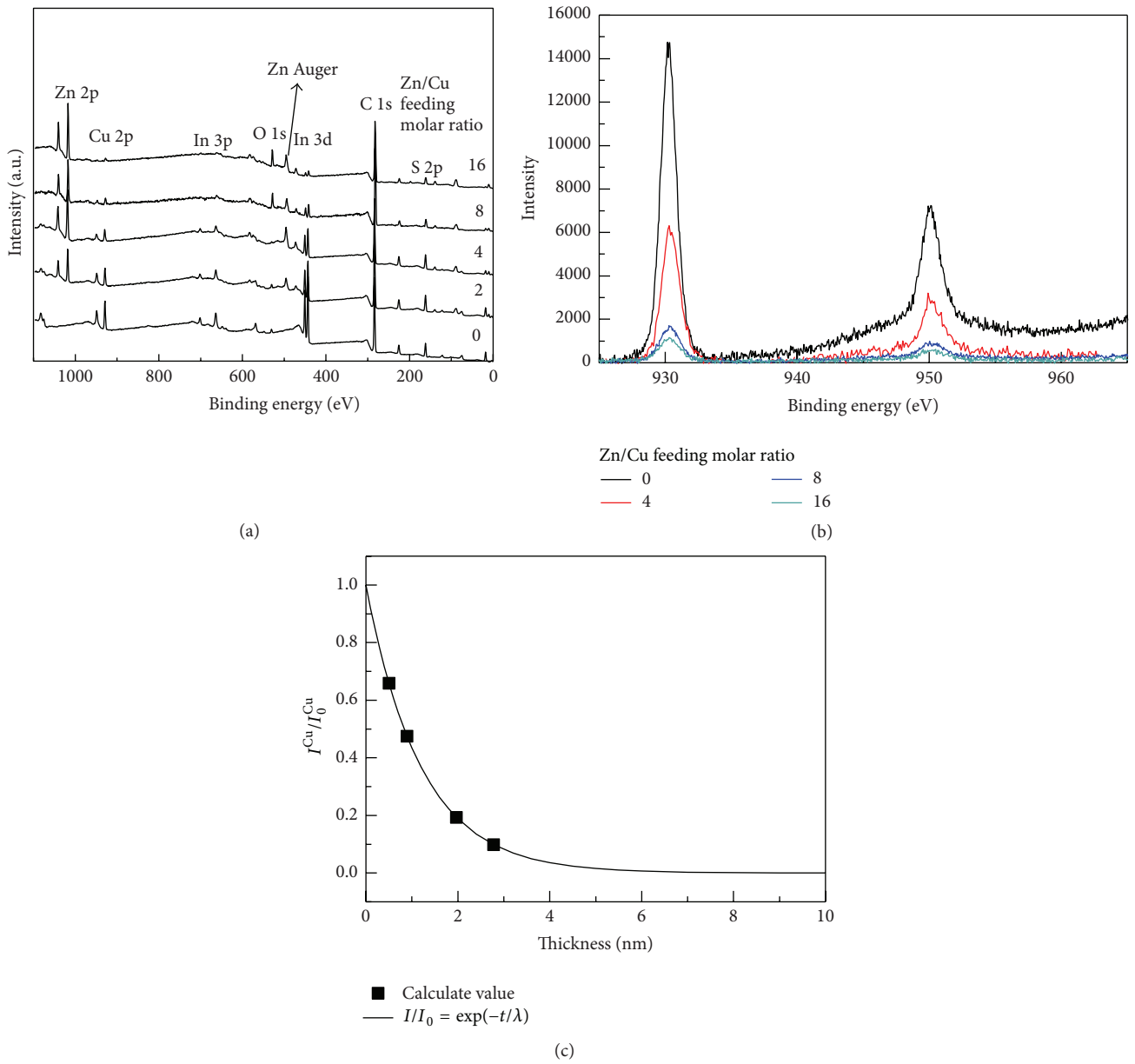

FIGURE 1: (a) XPS peaks from CIS and core/shell CIS/ZnS QDs with different Zn/Cu feeding molar ratios, (b) high resolution scans of Cu 2p photoelectrons, and (c) normalized intensity of the Cu 2p peak versus ZnS shell thickness. The solid line is an exponential attenuation curve based on a ZnS photoelectron escape distance of 1.2 nm. The calculated averages of ZnS shell thickness are 0.5, 0.9, 2.4, and 2.8 nm with Zn/Cu feeding molar ratios of 2, 4, 8, and 16, respectively.

[10, 29, 37, 38]. It was proved that the epitaxial grown CIS/ZnS QDs had a gradient chemical composition between CIS core and ZnS shell (the so-called gradient core/shell CIS/ZnS). The thickness calculated by XPS obviously includes not only ZnS but also gradient layers.

On the basis of the discussion, we can trace the growth mechanism of gradient core/shell CIS/ZnS QDs as follows (Figure 4): CuAc, $In(Ac)_3$, and DDT initially reacted to form CIS QDs as $Zn(Ac)_2$ and DDT were added; ZnS was coated on the surface of CIS QDs with prolonged shell growth time to form a ZnS layer accompanied with the gradual replacement of In^{3+} by Zn^{2+} on the surface and forming gradient $ZnCuInS_2$ (Zn-CIS) layers. As the shell growth time was prolonged, more ZnS was deposited on the surface of QDs and the thickness of Zn-CIS layer increased due to continuous replacement of Zn^{2+}. Finally, gradient core/shell CIS/ZnS QDs formed with the shrinked core size.

The crystal phase of obtained QDs was measured by XRD. Figure 5 shows the XRD patterns of prepared samples with Zn/Cu feeding molar ratios in the range of 0~16. The bare CIS QDs prepared exhibited three broad peaks at 2θ = 27.87°, 46.23°, and 55.08°, which were assigned to diffractions of the (112), (204), and (312) planes of chalcopyrite CIS crystal, respectively [30]. After shell growth, the above three

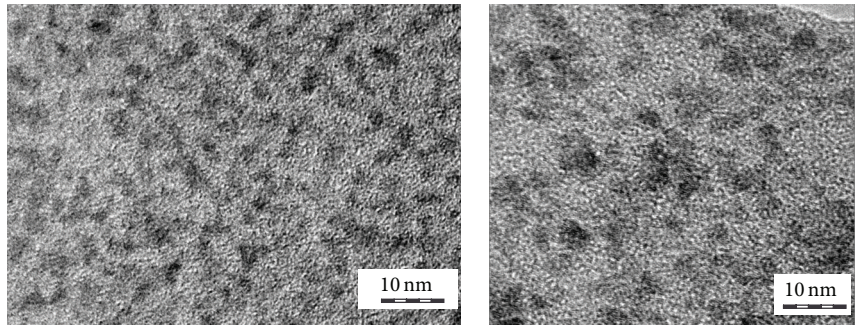

Figure 2: TEM images of (a) 60 min grown CIS QDs at 240°C, and (b) CIS/ZnS QDs with a core reaction time of 60 min at 240°C and a shell growth time of 60 min at 240°C. Zn/Cu feeding molar ratio was 4. The mean diameter of bare CIS is 3.3 nm, and CIS/ZnS QDs have a mean diameter of 4.3 nm.

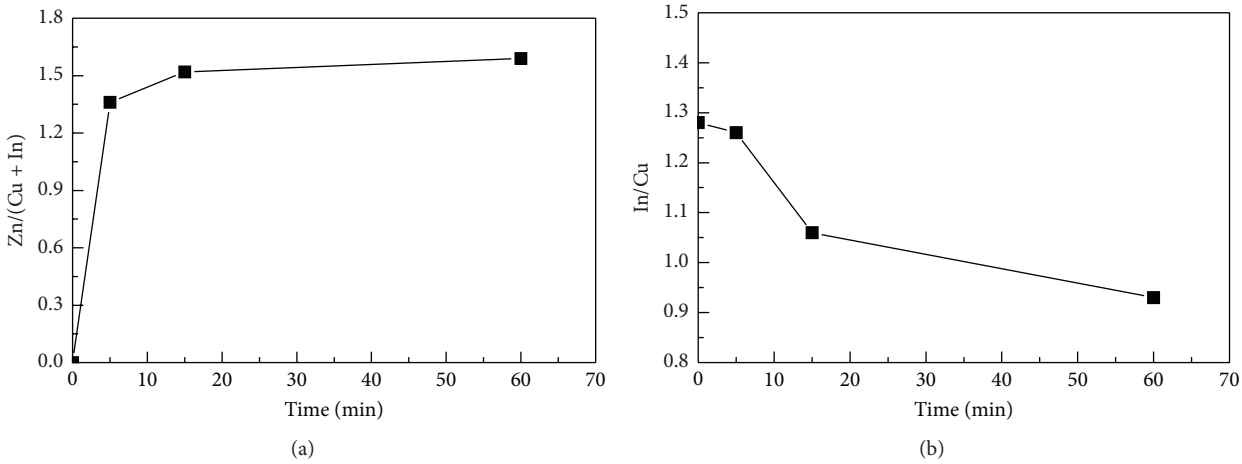

Figure 3: (a) Zn/(Cu + In) and (b) In/Cu atomic ratio changes with shell growth time. CIS QDs were prepared at 240°C for 60 min; and ZnS shell was grown at 240°C for 0~60 min with Zn/Cu feeding molar ratio of 4. The atomic concentration in nanocrystals was tested by ICP-OES.

broad peaks can still be observed, and each peak was located between the peaks for bulk zinc blend ZnS and chalcopyrite CIS. In addition, all of the peaks exhibited a shift to larger angles with an increase of the Zn/Cu molar ratio in the feed. This indicated that the fraction of ZnS inflated with increase of Zn/Cu feeding molar ratio. The diffraction peaks shifted to high 2θ angles because of the strain from epitaxial growth of ZnS on a CIS core.

In accordance with the size-dependent properties of semiconductors, the growth of ZnS influenced PL wavelengths and intensities. Figures 6(a) and 6(b) display the UV-vis absorption and PL behavior of as-prepared CIS and gradient core/shell CIS/ZnS QDs dispersed in a toluene solution. CIS cores were synthesized at a fixed temperature of 240°C for 60 min. Similar with previously reported results for I-III-VI group QDs [27, 32], the absorption spectrum has no obvious absorption peaks like traditional binary QDs such as CdSe [39, 40]. The PL spectrum displayed a broad emission bandwidth (FWHM) of 90~110 nm. The QY of obtained CIS QDs was 5.7%. The epitaxial growth of shell ZnS was kept at 240°C for 5~120 min based on the obtained CIS solution. As shown in Figure 6(b), the growth of ZnS on CIS core QDs resulted in a significant enhancement of the PL intensity. As the time of the shell growth varied from 5 to 180 min, the PL intensity and QY increased to a maximum value of 80% at 90 min. At longer times, QY slightly declined to 75% at 180 min (Figure 6(c)). The dramatic improvement of PL intensity is because the reduction of surface defects (S'', $In^{\bullet\bullet\bullet}$, $In_{Cu}{}''$, In''', Cu', $In_{Cu}{}^{\bullet\bullet}$, Cu'', etc.) acted as traps by the ZnS shell. Therefore, the elimination of defects minimizes the probability of undesired nonradiative and donor-acceptor pair recombination [22, 23, 41, 42]. The increase of the PL intensity and of QY with growth time of shell could be rationalized by the growth of ZnS supported by the gradual release of S from decomposition of DDT. Since DDT acted as capping ligands on surface layer in addition to being a S source. At very long time (>90 min), DDT on the surface of CIS/ZnS QDs was decomposed gradually and new defects were probably generated, causing the slight decrease of QY.

It is noted that the emission spectrum of CIS/ZnS QDs had a continuous blue shift that increased with growth time of the shell. The CIS/ZnS QDs exhibited a dramatic blue shift

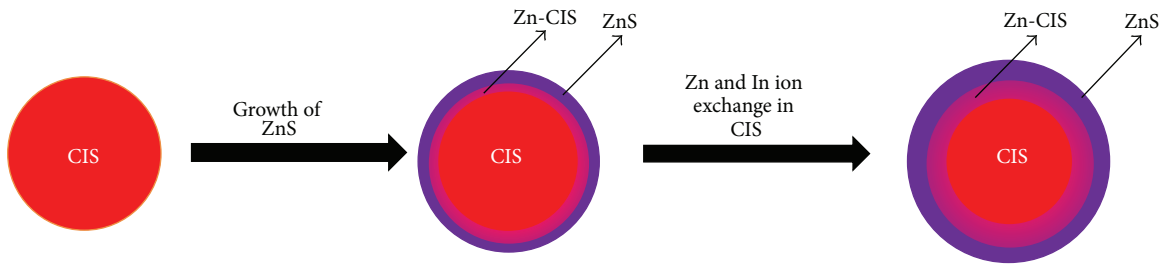

Figure 4: Schematic of the possible reaction mechanism for gradient core/shell CIS/ZnS QDs synthesis.

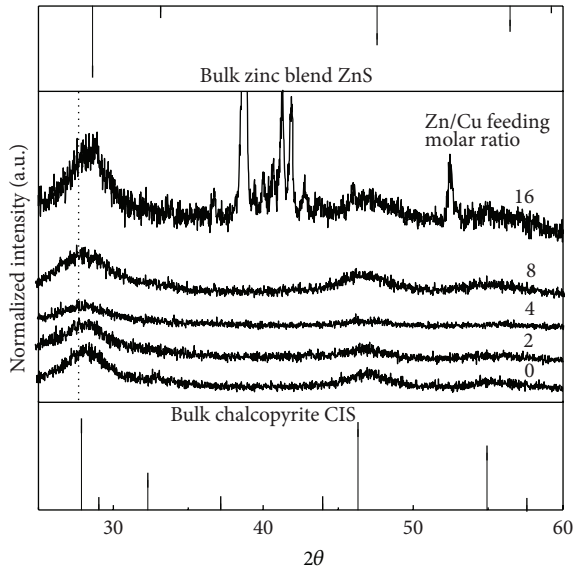

Figure 5: XRD patterns of prepared samples with different Zn/Cu feeding molar ratios. Reference patterns of bulk zinc blend ZnS and chalcopyrite CIS are also shown at the top and bottom, respectively [30, 31]. CIS QDs were prepared at 240°C for 60 min; growth of ZnS was at 240°C for 180 min.

of 37 nm from 654 nm for a bare CIS to 617 nm for core/shell QDs after 5 min of shell growth and to 580 nm after 180 min. The blue shift can be attributed to the combined effects of surface passivation by ZnS as well as the shrinking of CIS core. Surface passivation by ZnS induced the elimination or reduction of nonradiative transition and donor-acceptor emission with low energy level. The increased fraction of free-to-bound emissions with high energy level during the gradual surface passivation of CIS is one of the reasons for blue shift of PL spectrum. At the beginning of shell growth, a dramatic blue shift of PL wavelength is the main contribution of ZnS passivation. The Zn^{2+}/In^{3+} ion exchange caused shrinking of CIS core as the shell grew at temperature above 200°C, which is another reason for the continuous blue shift of the PL wavelength. The PL properties of CIS/ZnS QDs also supported our hypothesis of gradient core/shell structures. The gradient of the chemical composition between CIS core and ZnS shell decreases also their lattice mismatch. In turn, crystal defects can be minimized and the high QY could be reached. A series of gradient core/shell CIS/ZnS QDs can be tuned to emit in the 560–710 nm range through adjustment of the shell growth time (Figure 7). The effects of other parameters such as Zn/Cu feeding molar ratio and shell growth temperature on emission properties will be discussed and presented elsewhere.

The growth of core/shell nanocrystals improved not only the PL efficiency of the CIS QDs but also their photostability. The prepared CIS and CIS/ZnS QDs were stored in ambient condition without any inert protection. The PL QY changes of the samples were monitored under different storage time. As shown in Figure 8, QY of the fresh prepared CIS decreased from 9% to 2% after 1 month and to zero after two years, which indicated the unstable properties of CIS to air. However, QY of as-prepared CIS/ZnS QDs has only slightly decreased from 80% to 79% after 1 month and stayed at 72% two years later. It indicated that the ZnS surface on CIS will keep it from oxidizing. The high photostability of CIS/ZnS QDs promotes the potential in photovoltaic applications.

4. Conclusions

In summary, a simple method for synthesis of gradient core/shell CIS/ZnS QDs with high photoluminescence was developed using zinc acetate as Zn source and DDT both as S source and ligands at high temperatures for shell growth. The structure obtained QDs were traced as a core/shell structure

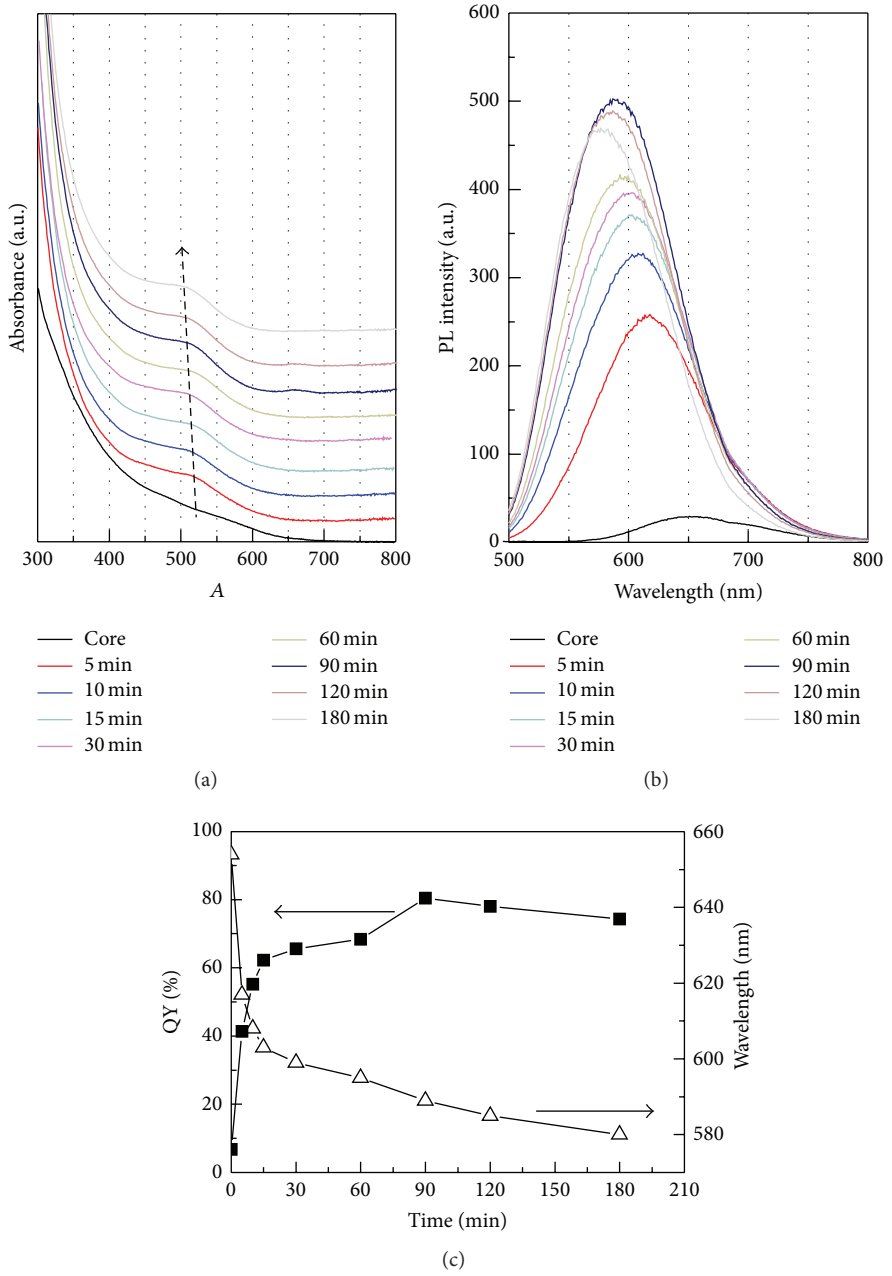

Figure 6: Temporal evolution of (a) absorption spectra, (b) PL spectra, and (c) QY and PL emission wavelength of as-prepared gradient core/shell CIS/ZnS QDs. CIS cores were synthesized at 240°C for 60 min. CIS/ZnS QDs were synthesized at shell growth temperature of 240°C and Zn/Cu feeding molar ratio of 4. The ZnS shell growth time was ranged from 5 min to 180 min.

with a gradient chemical composition between CIS core and ZnS shell by ICP-OES, XPS, and TEM analysis. The crystal phase of CIS was tetragonal chalcopyrite and the ZnS growth at high temperature did not affect the phase structure of CIS based on XRD analysis. PL QY of CIS QDs was increased to above 80% due to the ZnS shell. The growth of the shell caused reduction of the surface defects and minimized nonradiative emission. The obtained gradient core/shell CIS/ZnS QDs exhibit high PL intensity and quantum yield due to the gradient in the chemical composition between CIS core and ZnS shell, which effectively decreases their lattice mismatch. The PL emission can be tuned in the range of 560–710 nm by adjusting shell growth time. The prepared CIS/ZnS QDs have high photostability in ambient condition since ZnS surface can keep QDs from oxidizing.

Conflict of Interests

The authors declare that there is no conflict of interests regarding the publication of this paper.

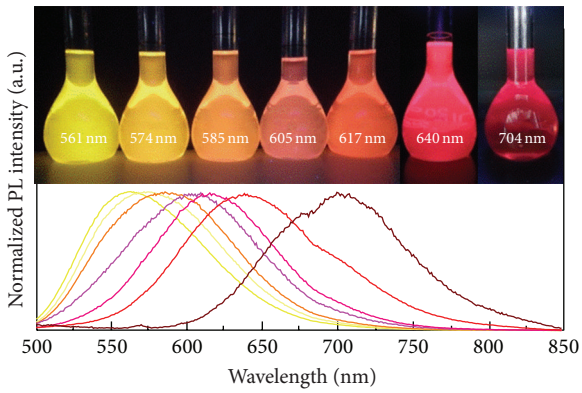

Figure 7: PL spectra (bottom) and photograph (top) of CIS-based samples irradiated by UV light (365 nm). The samples were diluted in toluene.

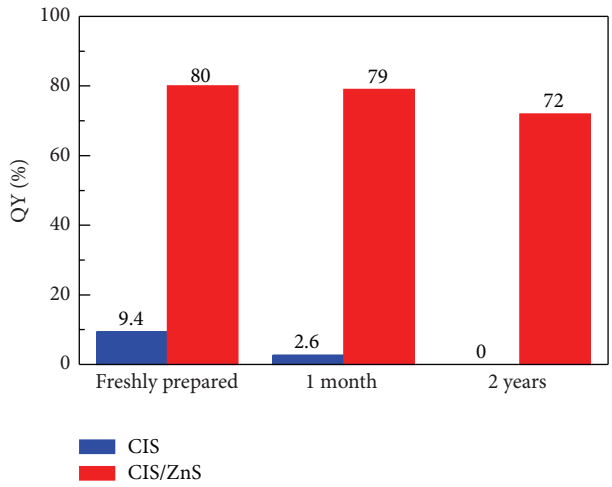

Figure 8: PL QY evolution of CIS and CIS/ZnS QDs when freshly prepared, after one month, and again after two years.

Acknowledgments

This work was financially supported by the National Nature Science Foundation of China (51172072), the Fundamental Research Funds for the Central Universities (WJ0913001), the State Key Laboratory of Chemical Engineering at ECUST (SKL-ChE-08C09), Bayer Technology & Engineering (Shanghai) Co. Ltd., and Bayer Technology Services GmbH. The authors are grateful to Dr. Frank Rauscher and Dr. Hua-Chang Lu for their help in the experiments and kind discussion. The authors are grateful to Dr. Werner Hoheisel for their help with respect to photoluminescence spectra analysis. The authors are also grateful to Dr. Dieter Heinz and Dr. Tao Liu for the time support.

References

[1] K. Zhao, Z. X. Pan, I. Mora-Sero et al., "Boosting power conversion efficiencies of quantum-dot-sensitized solar cells beyond 8% by recombination control," *Journal of the American Chemical Society*, vol. 137, no. 16, pp. 5602–5609, 2015.

[2] J. Schornbaum, Y. Zakharko, M. Held, S. Thiemann, F. Gannott, and J. Zaumseil, "Light-emitting quantum dot transistors: emission at high charge carrier densities," *Nano Letters*, vol. 15, no. 3, pp. 1822–1828, 2015.

[3] Z. L. Zhang, D. Liu, D. Z. Li et al., "Dual emissive Cu:InP/ZnS/InP/ZnS nanocrystals: single-source 'Greener' emitters with flexibly tunable emission from visible to near-infrared and their application in white light-emitting diodes," *Chemistry of Materials*, vol. 27, no. 4, pp. 1405–1411, 2015.

[4] X. B. Wang, W. W. Li, and K. Sun, "Stable efficient CdSe/CdS/ZnS core/multi-shell nanophosphors fabricated through a phosphine-free route for white light-emitting-diodes with high color rendering properties," *Journal of Materials Chemistry*, vol. 21, no. 24, pp. 8558–8565, 2011.

[5] W.-K. Lee, S. J. Hwang, M.-J. Cho et al., "CIS–ZnS quantum dots for self-aligned liquid crystal molecules with superior electro-optic properties," *Nanoscale*, vol. 5, no. 1, pp. 193–199, 2013.

[6] G. Konstantatos and E. H. Sargent, "Solution-processed quantum dot photodetectors," *Proceedings of the IEEE*, vol. 97, no. 10, pp. 1666–1683, 2009.

[7] T. Sun, K. Li, Y. P. Li et al., "Optimizing conditions for encapsulation of QDs by varying PEG chain density of amphiphilic centipede-like copolymer coating and exploration of QDs probes for tumor cell targeting and tracking," *New Journal of Chemistry*, vol. 36, no. 11, pp. 2383–2391, 2012.

[8] W. Luan, H. Yang, Z. Wan, B. X. Yuan, X. H. Yu, and S. T. Tu, "Mercaptopropionic acid capped CdSe/ZnS quantum dots as fluorescence probe for lead(II)," *Journal of Nanoparticle Research*, vol. 14, no. 3, 2012.

[9] S.-T. Tu, X. H. Yu, W. L. Luan, and H. Loewe, "Development of micro chemical, biological and thermal systems in China: a review," *Chemical Engineering Journal*, vol. 163, no. 3, pp. 165–179, 2010.

[10] W. S. Guo, N. chen, Y. Tu et al., "Synthesis of Zn-Cu-In-S/ZnS core/shell quantum dots with inhibited blue-shift photoluminescence and applications for tumor targeted bioimaging," *Theranostics*, vol. 3, no. 2, pp. 99–108, 2013.

[11] S. D. Chang, M. Zhou, and C. P. Grover, "Information coding and retrieving using fluorescent semiconductor nanocrystals for object identification," *Optics Express*, vol. 12, no. 1, pp. 143–148, 2004.

[12] V. I. Klimov, A. A. Mikhailovsky, S. Xu et al., "Optical gain and stimulated emission in nanocrystal quantum dots," *Science*, vol. 290, no. 5490, pp. 314–317, 2000.

[13] M. Kazes, D. Y. Lewis, Y. Ebenstein, T. Mokari, and U. Banin, "Lasing from semiconductor quantum rods in a cylindrical microcavity," *Advanced Materials*, vol. 14, pp. 317–321, 2002.

[14] A. V. Malko, A. A. Mikhailovsky, M. A. Petruska et al., "From amplified spontaneous emission to microring lasing using nanocrystal quantum dot solids," *Applied Physics Letters*, vol. 81, no. 7, pp. 1303–1305, 2002.

[15] J. D. Olson, G. P. Gray, and S. A. Carter, "Optimizing hybrid photovoltaics through annealing and ligand choice," *Solar Energy Materials and Solar Cells*, vol. 93, no. 4, pp. 519–523, 2009.

[16] C. S. Ferekides, D. Marinskiy, V. Viswanathan et al., "High efficiency CSS CdTe solar cells," *Thin Solid Films*, vol. 361, pp. 520–526, 2000.

[17] J. S. Steckel, J. P. Zimmer, S. Coe-Sullivan, N. E. Stott, V. Bulović, and M. G. Bawendi, "Blue luminescence from (CdS)ZnS core-shell nanocrystals," *Angewandte Chemie—International Edition*, vol. 43, no. 16, pp. 2154–2158, 2004.

[18] J. J. Choi, Y.-F. Lim, M. B. Santiago-Berrios et al., "PbSe nanocrystal excitonic solar cells," *Nano Letters*, vol. 9, no. 11, pp. 3749–3755, 2009.

[19] B. X. Yuan, W. L. Luan, and S.-T. Tu, "One-step synthesis of cubic FeS_2 and flower-like $FeSe_2$ particles by a solvothermal reduction process," *Dalton Transactions*, vol. 41, no. 3, pp. 772–776, 2012.

[20] T. Watanabe, H. Nakazawa, and M. Matsui, "Improvement of the electrical properties of Cu-poor $CuInS_2$ thin films by sodium incorporation," *Japanese Journal of Applied Physics*, vol. 37, pp. 1370–1372, 1998.

[21] T. Pons, E. E. Pic, N. Lequeux et al., "Cadmium-free $CuInS_2$/ZnS quantum dots for sentinel lymph node imaging with reduced toxicity," *ACS Nano*, vol. 4, no. 5, pp. 2531–2538, 2010.

[22] M. V. Yakushev, A. V. Mudryi, I. V. Victorov, J. Krustok, and E. Mellikov, "Energy of excitons in $CuInS_2$ single crystals," *Applied Physics Letters*, vol. 88, Article ID 011922, 2006.

[23] J. Hofhuis, J. Schoonman, and A. Goossens, "Elucidation of the excited-state dynamics in $CuInS_2$ thin films," *Journal of Physical Chemistry C*, vol. 112, no. 38, pp. 15052–15059, 2008.

[24] J. B. Zhang, W. P. Sun, L. P. Yin, X. S. Miao, and D. L. Zhang, "One-pot synthesis of hydrophilic $CuInS_2$ and $CuInS_2$–ZnS colloidal," *Journal of Materials Chemistry C*, vol. 2, pp. 4812–4817, 2014.

[25] R. G. Xie, M. Rutherford, and X. G. Peng, "Formation of high-quality I-III-VI semiconductor nanocrystals by tuning relative reactivity of cationic precursors," *Journal of the American Chemical Society*, vol. 131, no. 15, pp. 5691–5697, 2009.

[26] X. S. Tang, W. L. Cheng, E. S. G. Choo, and J. M. Xue, "Synthesis of CuInS2-ZnS alloyed nanocubes with high luminescence," *Chemical Communications*, vol. 47, no. 18, pp. 5217–5219, 2011.

[27] L. Li, T. J. Daou, I. Texier, T. T. K. Chi, N. Q. Liem, and P. Reiss, "Highly luminescent $CuInS_2$/ZnS Core/Shell nanocrystals: cadmium-free quantum dots for in vivo imaging," *Chemistry of Materials*, vol. 21, no. 12, pp. 2422–2429, 2009.

[28] L. Li, A. Pandey, D. J. Werder, B. P. Khanal, J. M. Pietryga, and V. I. Klimov, "Efficient synthesis of highly luminescent copper indium sulfide-based core/shell nanocrystals with surprisingly long-lived emission," *Journal of the American Chemical Society*, vol. 133, no. 5, pp. 1176–1179, 2011.

[29] J. Park and S.-W. Kim, "$CuInS_2$/ZnS core/shell quantum dots by cation exchange and their blue-shifted photoluminescence," *Journal of Materials Chemistry*, vol. 21, no. 11, pp. 3745–3750, 2011.

[30] *Bulk Chalcopyrite CIS Power Diffraction File*, JCPDS: 65-2372.

[31] *Bulk Zinc Blend ZnS Power Diffraction File*, JCPDS: 05-0566.

[32] H. Z. Zhong, Y. Zhou, M. F. Ye et al., "Controlled synthesis and optical properties of colloidal ternary chalcogenide CuInS2 nanocrystals," *Chemistry of Materials*, vol. 20, no. 20, pp. 6434–6443, 2008.

[33] D.-E. Nam, W.-S. Song, and H. Yang, "Facile, air-insensitive solvothermal synthesis of emission-tunable $CuInS_2$/ZnS quantum dots with high quantum yields," *Journal of Materials Chemistry*, vol. 21, no. 45, pp. 18220–18226, 2011.

[34] J. Choi, T.-K. Tseng, M. Davidson, and P. H. Holloway, "Enhanced photoluminescence from Gd_2O_3:Eu^{3+} nanocores with a Y_2O_3 thin shell," *Journal of Materials Chemistry*, vol. 21, no. 9, pp. 3113–3118, 2011.

[35] H. Borchert, S. Haubold, M. Haase et al., "Investigation of ZnS passivated in P nanocrystals by XPS," *Nano Letters*, vol. 2, no. 2, pp. 151–154, 2002.

[36] S. Tanuma, C. J. Powell, and D. R. Penn, "Calculations of electron inelastic mean free paths. III. Data for 15 inorganic compounds over the 50–2000 eV range," *Surface and Interface Analysis*, vol. 17, no. 13, pp. 927–939, 1991.

[37] H. Wiedemeier and R. Z. Santandrea, "Mass spectrometric studies of the decomposition and the heat of formation of $CuInS_2$(s)," *Zeitschrift für Anorganische und Allgemeine Chemie*, vol. 497, no. 2, pp. 105–118, 1983.

[38] S. Deore and A. Navrotsky, "Oxide melt solution calorimetry of sulfides: enthalpy of formation of sphalerite, galena, greenockite, and hawleyite," *American Mineralogist*, vol. 91, no. 2-3, pp. 400–403, 2006.

[39] H. W. Yang, W. L. Luan, S.-T. Tu, and Z. M. Wang, "High-temperature synthesis of CdSe nanocrystals in a serpentine microchannel: wide size tunability achieved under a short residence time," *Crystal Growth and Design*, vol. 9, no. 3, pp. 1569–1574, 2009.

[40] W. L. Luan, H. W. Yang, S. T. Tu, and Z. M. Wang, "Open-to-air synthesis of monodisperse CdSe nanocrystals via microfluidic reaction and its kinetics," *Nanotechnology*, vol. 18, Article ID 175603, 2007.

[41] J. Krustok, J. Raudoja, and H. Collan, "Photoluminescence and the tetragonal distortion in $CuInS_2$," *Thin Solid Films*, vol. 387, no. 1-2, pp. 195–197, 2001.

[42] S. L. Castro, S. G. Bailey, R. P. Raffaelle, K. K. Banger, and A. F. Hepp, "Synthesis and characterization of colloidal $CuInS_2$ nanoparticles from a molecular single-source precursor," *Journal of Physical Chemistry B*, vol. 108, no. 33, pp. 12429–12435, 2004.

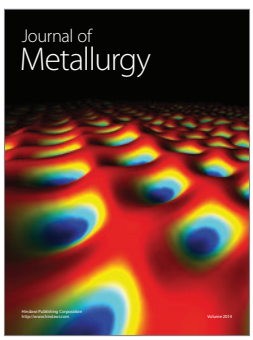

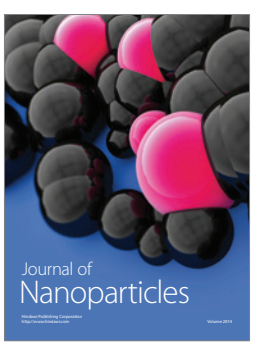

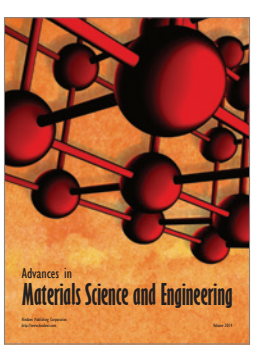

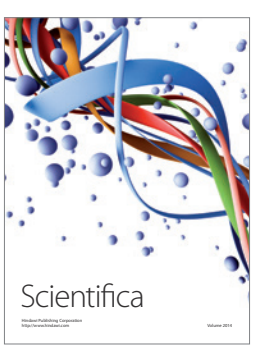

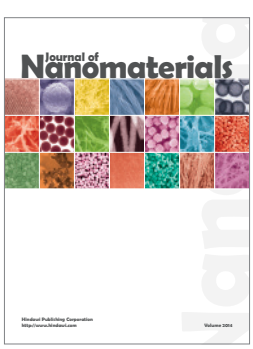

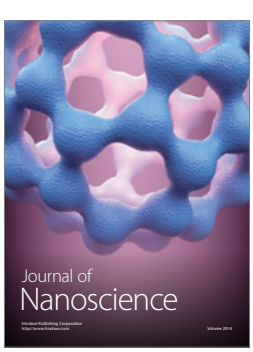

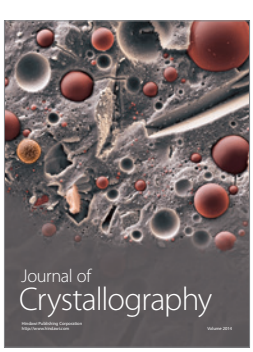

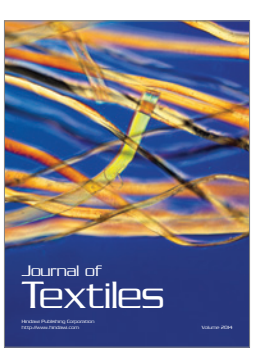

Hindawi

Submit your manuscripts at
http://www.hindawi.com